

# Evidence for the surface-diffusion mechanism of solution crystallization from molecular-level observations with ferritin

Kai Chen<sup>1</sup> and Peter G. Vekilov<sup>2</sup><sup>1</sup>Center for Microgravity and Materials Research, University of Alabama in Huntsville, Huntsville, Alabama 35899<sup>2</sup>Department of Chemical Engineering, University of Houston, Houston, Texas 77204

(Received 19 April 2002; published 28 August 2002)

We employ atomic force microscopy to monitor *in situ*, in real time, the molecular processes of crystallization of ferritin, a protein that has an inorganic single-crystalline core that can be varied. We determine the statistics of molecular attachment and detachment at the growth sites and find that the ratio of the fluxes in and out of the kinks is significantly lower than expected, assuming direct incorporation of the molecules from the solution. Determinations of the energy barrier for incorporation yield  $\sim 30 \text{ kJ mol}^{-1}$ , significantly higher than expected for this mechanism. We conclude that attachment of molecules occurs via the surface adsorption layer. The surface coverage resulting from this mechanism is  $\sim 0.9$ , suggesting a growth mode different from the classical surface diffusion mechanism.

DOI: 10.1103/PhysRevE.66.021606

PACS number(s): 81.10.-h, 82.20.Yn, 82.39.Rt

## I. INTRODUCTION

During crystal growth from solution, the growth sites, the kinks, are for many systems located along the edges of the unfinished crystal layers, the steps [1]. The solute molecules have two possible pathways between the solution and the kinks: they can be directly incorporated [2,3], or they can first adsorb on the terraces between the steps, diffuse along them, and then reach the steps [2,4].

If a crystal grows by the direct incorporation mechanism, the competition for supply between adjacent steps is mild [3]. On the contrary, competition for supply confined to the adsorption phase is acute [5]; it retards step propagation and acts as a strong effective attraction between the steps. This dramatically affects the stability of the step train, the appearance and evolution of step bunches [6], and, ultimately, the crystal quality and utility [7].

The two mechanisms can be directly discerned by monitoring the adsorbed solute molecules on the crystal surface, similarly to experiments with metal atoms at lowered temperatures [8]. However, during solution growth at room temperature, the diffusivity of the adsorbed species is  $\sim 10^{-8} \text{ cm}^2 \text{ s}^{-1}$  [9,10], i.e., a molecule passes 100 nm in  $\sim 0.01 \text{ s}$ . With *in situ* atomic force microscopy, this distance is covered by the scanning tip typically in  $\sim 0.1 \text{ s}$ , i.e., imaging is too slow to detect and monitor the adsorbed molecules. Electron microscopy of flash-frozen samples has in several cases revealed the presence of adsorbed solute molecules on the crystal surface [11]; however, their participation in growth cannot be confidently judged by this technique. As direct tests appear impossible, indirect evidence for the growth mechanism of several systems has been sought.

For several solution-grown crystals, the growth mechanism has been deduced by comparing the velocities of isolated steps to those of closely spaced steps. Similar values of the two velocities for silver [12] and calcite [13] were taken as evidence of the direct incorporation mechanism. Conversely, slower growth of dense step segments was

interpreted in favor of the surface diffusion mechanism for potassium dihydrogen phosphate/ammonium dihydrogen phosphate [9,14], lysozyme [15], and canavalin [10]. A known problem for such mesoscale data is that the data sets interpreted in favor of direct incorporation could also reflect a surface diffusion range shorter than the shortest step separation probed [13]. Thus, critical evidence about the growth mode should be sought by studying the growth processes at the molecular level [16,17].

As an example of such tests, we use the crystallization of the protein ferritin, which has molecules that are quasispherical and crystallize in a face-centered-cubic (fcc) lattice [18]. Besides being a rather convenient model system, ferritin is a workhorse in several research areas: nanoassembly, drug delivery, biomineralization, etc. The iron-containing core of ferritin can be replaced with other organic, inorganic, and bio-organic compounds for various applications in these areas [19]. Octahedral {111} faces dominate the crystal habit. Growth from solution purified by gel filtration [20] occurs by the spreading of layers generated by surface nucleation. The steps interact at separations  $< 10$  molecular sizes [16,17]. However, the interaction is mostly repulsive [21] and has been attributed to loss of configurational entropy due to geometric constraints imposed by the close spacing [6]; at longer separations, the steps do not interact.

## II. METHODS

We used atomic force microscopy with tapping imaging mode for *in situ* monitoring of the crystallization processes. With the ferritin system, this allows submolecular resolution of about  $16 \text{ \AA}$  [17]; the crystallization conditions and all other experimental details were as in Refs. [17,22]. The solubility of ferritin  $C_e = 35 \mu\text{g mL}^{-1}$ . For the investigations of the temperature effects, we mounted the sample onto a Peltier-cooled disk firmly attached to the scanner. This allowed imaging in the range of  $28\text{--}45 \text{ }^\circ\text{C}$ ; to access  $25 \text{ }^\circ\text{C}$  and  $20 \text{ }^\circ\text{C}$ , the room temperature was set to  $18\text{--}20 \text{ }^\circ\text{C}$ .

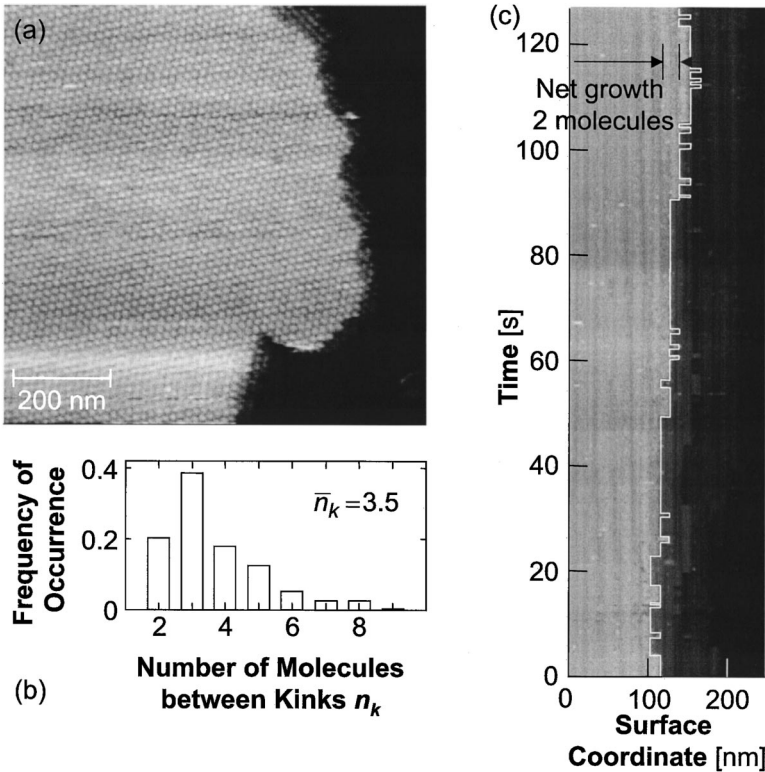


FIG. 1. The molecular mechanism of crystallization of ferritin. Brighter gray shades correspond to higher locations. (a) Growth step at  $C = 70 \mu\text{g cm}^{-3}$ ,  $(C/C_e - 1) = 1$ . Chosen contrast setting hides the molecular structure of the lower layer. (b) Distribution of molecules between kinks on steps located  $\sim 0.5 \mu\text{m}$  apart, obtained from images similar to (a) at the same  $(C/C_e - 1)$ . (c) Incorporation of molecules into steps at  $(C/C_e - 1) = 1$ . A pseudotime recorded with the scan axis parallel to the step disabled at time  $= 0$ , as in Refs. [16,17], shows displacement of one molecular site at the step. White contour traces step position. Shifts of this contour to the right correspond to molecules attaching to the monitored site, shifts to the left reflect detachments of molecules; the number of such shifts and the time of monitoring, 128 s, are used to determine  $j_+/j_-$  and  $(j_+ - j_-)$ , as in Refs. [16,17].

### III. RESULTS

To characterize the molecular-level growth mechanism of the ferritin crystals, we imaged the step structure, and monitored the flux of molecules into the step, as done before for apoferritin [16,17]. Figure 1(a) demonstrates the characteristic roughness of the growth steps on a ferritin crystal. Figure 1(b) shows the distribution of  $n_k$ , the separation between the kinks. The mean  $\bar{n}_k = 3.5$ , corresponding to mean kink density  $\bar{n}_k^{-1} = 0.28$ . Similar data at other ferritin concentrations  $C$  and temperatures  $T$  suggest that  $\bar{n}_k$  may be a weak function of  $T$ , and does not depend on  $C$ .

Figure 1(c) shows a pseudotime recorded with disabled scanning along the  $y$  axis so that the vertical coordinate becomes the time axis. To test if imaging in this mode does not affect the molecular attachment, as in Ref. [16], we performed an area scan that includes the line along which the disabled  $y$ -axis scan occurred, immediately after the data collection in Fig. 1(c) ended. The respective image (not shown) revealed that step motion is not inhibited or accelerated at the location of scanning, i.e., the chosen scanning parameters ensured that step propagation was not affected by scanning over the same line for  $\sim 2$  min.

This type of data collection does not allow observations of the neighboring sites at the step. Hence, we cannot directly distinguish between molecules entering the line of observation due to molecular diffusion along the step, or to exchange with either the terrace between the steps or the adjacent solution. While the latter results in step propagation and growth, the former is a process that only involves rearrangement of molecules already belonging to the crystal and may not be associated with growth. Analyses of the time autocorrelation function of the step position [23], analogous

to those in Ref. [16], yielded an exponent of  $\frac{1}{3}$  for the larger part of the data, indicating that the trace in Fig. 1(c) predominantly reflects the exchange of molecules between the step and its environment.

The net growth is two molecules for 128 s, leading to an average net flux  $(j_+ - j_-) = 0.054 \text{ s}^{-1}$  ( $j_+$  denotes attachment,  $j_-$  denotes detachment) into the growth sites distributed with mean density  $\bar{n}_k^{-1} = 0.28$ , the ratio  $j_+/j_- \leq 21/19 = 1.105$ . The  $\leq$  sign reflects the undetected pairs of attachment/detachment events separated by residence times shorter than the scanning period 0.5 s. Such misses do not affect the net flux  $(j_+ - j_-)$ . Since there are no sources or sinks of molecules at the step other than the attachment sites, the step growth rate  $v$  should equal  $a\bar{n}_k^{-1}(j_+ - j_-)$  [24,25], where  $a$  is the molecular size: for ferritin,  $a = 13 \text{ nm}$ . At  $(C/C_e - 1) = 1$ , at which all data in Fig. 1 were collected, the value of the step growth rate is  $v = 0.20 \text{ nm s}^{-1}$ , equal to the product  $a\bar{n}_k^{-1}(j_+ - j_-)$ . This equality indicates that the ferritin crystals grow by the attachment of single molecules to kinks located along the steps. Note that this equality is of limited significance. Thus, if the trace in Fig. 1(c) was interrupted at 120 s, the product  $a\bar{n}_k^{-1}(j_+ - j_-)$  would have been *higher* than the measured step velocity. While a lower product would indicate either insufficient statistics or tip impact in the disabled  $y$ -axis mode, higher values do not affect the conclusions reached.

In the case of direct incorporation from the solution [25,26],

$$j_+ - j_- = \nu_+ C_e \Omega \exp\left(-\frac{U_0}{k_B T}\right) \left[\frac{C}{C_e} - 1\right],$$

$$v_+ = \frac{D}{\Lambda a}, \text{ and } \frac{j_+}{j_-} = \frac{C}{C_e}. \quad (1)$$

Here,  $U_0$  is the energy barrier for incorporation into the kinks [3,24]; in the case of ferritin, it likely accounts for the need to expel the water molecules structured around hydrophilic patches on the surfaces of the incoming molecules and the molecules forming the kink [27].  $\Omega = 1.56 \times 10^{-18} \text{ cm}^3$  is the crystal volume per ferritin molecule,  $D = 3.2 \times 10^{-7} \text{ cm}^2 \text{ s}^{-1}$  is the ferritin diffusivity [28], and  $\Lambda$  is the radius of curvature of the surface-molecule interaction potential around its maximum at  $U_0$  [29], and, hence, should be of the order of a few water molecule sizes,  $\sim 5\text{--}10 \text{ \AA}$  [30]. The expression for the driving force  $(C/C_e - 1)$  relies on the fact that for the ferritin/apoferritin pair, the activity coefficients in the growth solution  $\gamma$  and at equilibrium  $\gamma_e$ ,  $\gamma \approx \gamma_e \approx 1$  [17]. The step velocity  $v$  for this growth mode is

$$v = \frac{a}{\bar{n}_k} (j_+ - j_-) = \frac{\Omega C_e D}{\bar{n}_k \Lambda} \exp\left(-\frac{U_0}{k_B T}\right) \left[\frac{C}{C_e} - 1\right]. \quad (2)$$

Analogous considerations for the case of growth via surface diffusion yield, for the net flux into the step from the surface,

$$j_{s+} - j_{s-} = v_{s+} n_e a^2 \exp\left(-\frac{U_{s0}}{k_B T}\right) \left[\frac{n_s}{n_e} - 1\right],$$

$$v_{s+} = \frac{D_s}{\Lambda_s a}, \text{ and } \frac{j_+}{j_-} = \frac{n_s}{n_e}, \quad (3)$$

where  $n_s$  and  $n_e$  are the surface concentration of adsorbed ferritin, and its equilibrium value, respectively;  $U_{s0}$  is the energy barrier for incorporation into the kink from the surface; and  $D_s$  and  $\Lambda_s$  are, respectively, the surface diffusivity and curvature of the surface  $U_s$ . For the step velocity, one gets through  $v = a/\bar{n}_k (j_{s+} - j_{s-})$  an expression analogous to Eq. (2).

Figure 1(c) reveals that at  $C/C_e = 2$ ,  $j_+/j_- \leq 1.105$ . For apoferritin, similar experiments have shown [16] that at  $C/C_e = 3$ ,  $j_+/j_- \leq 25/22 = 1.14$ . For both proteins, these ratios represent gross violations of the last equality of Eq. (1). These violations cannot be attributed to depletion of the solution layer adjacent to the crystal—this factor becomes significant at  $\sim 100\times$  (higher growth rates) [31]—and suggest that the direct incorporation mechanism may not apply. In the case of Langmuir adsorption,  $n_s = n_{s\infty} C/(B+C)^{-1}$  ( $B$  is the Langmuir constant) and  $n_s/n_e < C/C_e$ . Hence, the lower ratios of the in- to outflux are compatible with a mechanism of incorporation from the state of adsorption on the surface.

Estimates of the ratio  $n_s/n_{s\infty}$  using the  $j_+/j_-$  ratios above yield 0.82 at  $C = C_e$ , 0.9 at  $C = 2C_e$ , and 0.93 at  $C = 3C_e$ . Typically, in considerations of the surface diffusion mechanism, it is assumed that one adsorption site is equivalent to one lattice site so that  $n_s/n_{s\infty} = 1$  corresponds to a full crystal layer. If this were the case here it is unlikely that the closely packed adsorbed molecules would have the surface mobility required for growth. This contradiction suggests that the molecular adsorption sites are not the crystal lattice

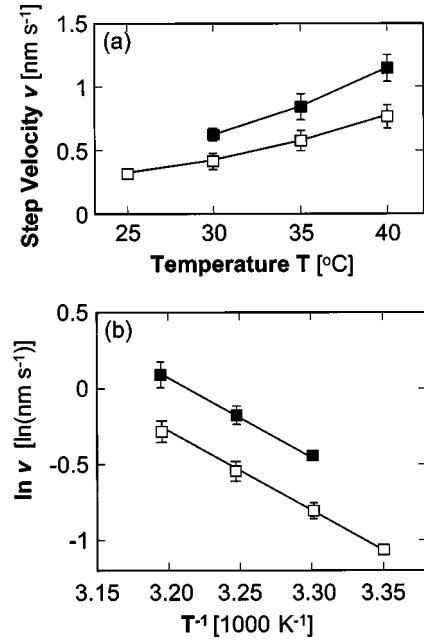


FIG. 2. Dependencies of the step velocity  $v$  for growth of ferritin on the temperature (a), and in Arrhenius coordinates (b). ■ at  $C/C_e = 4$ , □ at  $C/C_e = 3$ . For each point, positions of advancing steps were compared in sequences of molecular resolution *in-situ* antiferromagnetic images as in [16,17];  $\sim 20$  such determinations of  $v$  were averaged. The error bars represent the 90% confidence interval of the average [36].

sites in the layer under construction. The most likely candidates for adsorption sites are the three types of surface vacancies, discussed in Ref. [16]. As shown in [32], the surface density of these defects is up to 10%, with distances between them 2–5 molecular sizes. Note that assuming adsorption on such sites would require significant modifications in the surface diffusion model: (i) since their elastic energy varies [32], this would mean variable adsorption energy, contrary to a basic assumption of Langmuir adsorption; (ii) the exchange of molecules between the randomly distributed nonidentical sites may follow unusual statistics and dynamics. It is conceivable that the suspected unconventional adsorption state may be the main factor underlying the short surface diffusion range, discussed above.

For further tests of the growth mode, we examine the step velocity law in Eq. (2). The only unknown parameter here is the energy barrier  $U_0$ . Determinations of  $v$  at four temperatures and two ferritin concentrations in Fig. 2 yield  $E_{\text{total}} = 41 \pm 3 \text{ kJ mol}^{-1}$ . In Eq. (2),  $C_e$  [33] and  $\Omega$  do not depend on temperature, and  $\Lambda$  is about the size of a few water molecules and, in a first approximation, does not depend on  $T$  [30]. For a molecule following the Stokes law,  $D = D_0 \exp(-E_{\text{visc}}/k_B T)$ , where  $E_{\text{visc}}$  is the temperature factor in an Arrhenius-type expression for the dependence of the solvent viscosity on temperature. For NaCl solutions in Na acetate buffer, it is  $E_{\text{visc}} = 7.4 \text{ kJ mol}^{-1}$  [34]. As shown in [16],  $\bar{n}_k$  has a weak near-exponential dependence on  $T$  through the kink energy  $w = 3.8 \text{ kJ mol}^{-1}$ . This leaves  $U_0 \approx 30 \text{ kJ mol}^{-1}$ . This value is close to the  $28 \text{ kJ mol}^{-1}$  found as the average over systems ranging from inorganic salts,

through organics, to proteins and viruses [35].

Substituting into Eq. (2), we get at  $C/C_e=2$ ,  $v=0.0014 \text{ nm s}^{-1}$ , and at  $C/C_e=3$ ,  $v=0.0028 \text{ nm s}^{-1}$ . These values are more than two orders of magnitude lower than actually observed. The measured values of 0.20 and 0.31  $\text{nm s}$  would require  $U_0 \approx 18 \text{ kJ mol}^{-1}$ , beyond the range of the determination in Fig. 2. This discrepancy supports the assertion that the direct incorporation mechanism is inapplicable to the growth of ferritin. We conclude that a mechanism involving adsorption on the terraces better corresponds to the available data for ferritin. As noted above, in the ferritin/apoferritin system the steps do not exhibit attraction at any step separation. We conclude that to account for this the characteristic surface diffusion length [2] must be shorter than a few lattice parameters. Note that an investigation limited to data on the mesoscale step kinetics would have concluded that the growth mechanism is direct incorporation.

#### IV. DISCUSSION

A relevant question is why the energetics of the system select the surface diffusion mechanism over the direct incorporation. This question can only be addressed with the molecular-level data available for the system. We note that when the surface diffusion mechanism operates, the energy barrier determined from the data in Fig. 2 is a function of the barriers of the elementary steps of this mechanism and should be denoted as  $U_{\text{sum}}$ . As shown in [5,30],  $U_{\text{sum}} = U_{\text{ads}} - U_{\text{desorb}} + U_{\text{SD}} + U_{\text{step}}$ , which are the barriers, respectively, for adsorption, desorption, surface diffusion, and incorporation into the step, (Fig. 3). Since the energy effect of one intermolecular bond of ferritin should be equal to that of apoferritin,  $\phi = 3k_B T = 7.4 \text{ kJ mol}^{-1}$  [16], we can safely assume that for adsorption-desorption on a (111) fcc surface,  $U_{\text{ads}} - U_{\text{desorb}} = \Delta H_{\text{ads}} = -3\phi = -22 \text{ kJ mol}^{-1}$ . Ignoring interactions between the adsorbed molecules, the lowest possible value of  $U_{\text{SD}}$  occurs when only one bond is broken upon passage between two adsorption sites, hence  $U_{\text{SD}} \geq \phi$ .

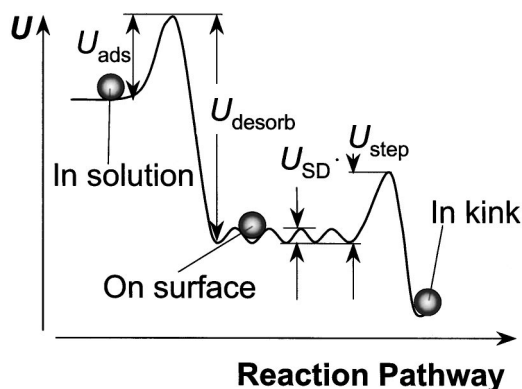


FIG. 3. The energy landscape of the surface diffusion mechanism. For notations, see text. Then see Ref. [37].

This yields  $U_{\text{step}} \leq 44 \text{ kJ mol}^{-1}$ , similar to the ammonium dihydrogen phosphate value [30]. Since an equal number of bonds—three—are created during adsorption and incorporation into the step, we can roughly assume  $U_{\text{ads}} \approx U_{\text{step}}$ . Thus, the highest barrier encountered by a molecule en route to the kink is  $\leq 44 \text{ kJ mol}^{-1}$ . For direct incorporation into kinks, for which all six bonds are created simultaneously,  $U_{\text{kink}} \sim U_{\text{ads}} + U_{\text{step}} \approx 88 \text{ kJ mol}^{-1}$ . A crude estimate yields that this would make growth via this pathway slower by a factor of  $\sim \exp[(88\,000 - 44\,000)/RT] \sim 10^8$ .

#### ACKNOWLEDGMENTS

We thank A. A. Chernov and D. N. Petsev for important suggestions, B. R. Thomas for the purified protein samples used in the experiments, S.-T. Yau and O. Galkin for help with the AFM technique, and N. A. Booth and O. Galkin for critical reading of the manuscript. This work was supported by the Office of Biological and Physical Sciences, NASA (Grant Nos. NAG8-1357 and NAG8-1824).

- 
- [1] W. Kossel, *Nachr. Ges. Wiss. Goettingen, Math.-Phys. Kl.* **135**, (1928).
- [2] W. K. Burton, N. Cabrera, and F. C. Frank, *Philos. Trans. R. Soc. London, Ser. A* **243**, 299 (1951).
- [3] A. A. Chernov, *Sov. Phys. Usp.* **4**, 116 (1961).
- [4] M. Volmer, *Kinetik der Phasenbildung* (Steinkopff, Dresden, 1939).
- [5] G. H. Gilmer, R. Ghez, and N. Cabrera, *J. Cryst. Growth* **8**, 79 (1971).
- [6] E. D. Williams and N. C. Bartelt, *Science* **251**, 393 (1991).
- [7] E. Bauser, in *Handbook of Crystal Growth*, edited by D. T. J. Hurle (North Holland, Amsterdam, 1984), Vol. 3b, p. 879.
- [8] G. Ehrlich and F. G. Hudda, *J. Chem. Phys.* **44**, 1039 (1966).
- [9] P. G. Vekilov, Y. G. Kuznetsov, and A. A. Chernov, *J. Cryst. Growth* **121**, 643 (1992).
- [10] T. A. Land, J. J. DeYoreo, and J. D. Lee, *Surf. Sci.* **384**, 136 (1997).
- [11] N. Braun, J. Tack, M. Fischer, A. Bacher, L. Bachmann, and S. Weinkauff, *J. Cryst. Growth* **212**, 270 (2000).
- [12] V. Bostanov, G. Staikov, and D. K. Roe, *J. Electrochem. Soc.* **122**, 1301 (1975).
- [13] A. J. Gratz, P. E. Hillner, and P. K. Hansma, *Geochim. Cosmochim. Acta* **57**, 491 (1993); P. E. Hillier, S. Manne, P. K. Hansma, and A. J. Gratz, *Faraday Discuss.* **95**, 191 (1993).
- [14] J. J. DeYoreo, T. A. Land, and B. Dair, *Phys. Rev. Lett.* **73**, 838 (1994).
- [15] P. G. Vekilov, L. A. Monaco, and F. Rosenberger, *J. Cryst. Growth* **156**, 267 (1995).
- [16] S.-T. Yau, B. R. Thomas, and P. G. Vekilov, *Phys. Rev. Lett.* **85**, 353 (2000).
- [17] S.-T. Yau, D. N. Petsev, B. R. Thomas, and P. G. Vekilov, *J. Mol. Biol.* **303**, 667 (2000).
- [18] W. H. Massover, *Micron* **24**, 389 (1993); P. M. Harrison and P. Arosio, *Biochim. Biophys. Acta* **1275**, 161 (1996).
- [19] S. Gider, D. D. Awschalom, T. Douglas, S. Mann, and M. Chaparala, *Science* **268**, 77 (1995); D. Yang and K. Nagayama,



- Biochem. J. **307**, 253 (1995).
- [20] B. R. Thomas, D. Carter, and F. Rosenberger, *J. Cryst. Growth* **187**, 499 (1997).
- [21] S.-T. Yau *et al.* (unpublished).
- [22] S.-T. Yau and P. G. Vekilov, *Nature (London)* **406**, 494 (2000).
- [23] M. Poensgen, J. Wolf, J. Frohn, M. Giesen, and H. Ibach, *Surf. Sci.* **274**, 430 (1992); L. Kuipers, M. Hoogeman, and J. Frenken, *Phys. Rev. Lett.* **71**, 3517 (1993); C. Alfonso, J. M. Bermond, J. C. Heyraud, and J. J. Metois, *Surf. Sci.* **262**, 371 (1992); N. C. Bartelt, T. L. Einstein, and E. D. Williams, *Surf. Sci. Lett.* **240**, L591 (1990); T. Ihle, C. Misbah, and O. Pierre-Louis, *Phys. Rev. B* **58**, 2289 (1998).
- [24] A. A. Chernov, *Modern Crystallography III, Crystal Growth* (Springer, Berlin, 1984).
- [25] A. A. Chernov and H. Komatsu, in *Science and Technology of Crystal Growth*, edited by J. P. van der Eerden and O. S. L. Bruinsma (Kluwer Academic, Dordrecht, 1995), p. 67.
- [26] A. A. Chernov and H. Komatsu, in *Science and Technology of Crystal Growth*, edited by J. P. van der Eerden and O. S. L. Bruinsma (Kluwer Academic, Dordrecht, 1995), p. 329.
- [27] D. N. Petsev and P. G. Vekilov, *Phys. Rev. Lett.* **84**, 1339 (2000).
- [28] D. N. Petsev, B. R. Thomas, S.-T. Yau, and P. G. Vekilov, *Biophys. J.* **78**, 2060 (2000).
- [29] M. Smoluchowski, *Phys. Z.* **17**, 557 (1916); H. Eyring, S. H. Lin, and S. M. Lin, *Basic Chemical Kinetics* (Wiley, New York, 1980).
- [30] P. G. Vekilov, Y. G. Kuznetsov, and A. A. Chernov, *J. Cryst. Growth* **121**, 44 (1992).
- [31] H. Lin, D. N. Petsev, S.-T. Yau, B. R. Thomas, and P. G. Vekilov, *Cryst. Growth and Design* **1**, 73 (2001).
- [32] S.-T. Yau, B. R. Thomas, O. Galkin, O. Gliko, and P. G. Vekilov, *Proteins: Struct., Funct., Genet.* **43**, 343 (2001).
- [33] D. N. Petsev, B. R. Thomas, S.-T. Yau, D. Tsekova, C. Nanev, W. W. Wilson, and P. G. Vekilov, *J. Cryst. Growth* **232**, 21 (2001).
- [34] W. J. Fredericks, M. C. Hammonds, S. B. Howard, and F. Rosenberger, *J. Cryst. Growth* **141**, 183 (1994).
- [35] J. J. DeYoreo, in *Thirteenth International Conference on Crystal Growth*, edited by T. Hibiya, J. B. Mullin, and M. Uwaha (Elsevier, Kyoto, Japan, 2001).
- [36] S. C. Choi, *Introductory Applied Statistics in Science* (Prentice Hall, Englewood Cliffs, NJ, 1978).
- [37] P. Bennema, *J. Cryst. Growth* **1**, 278 (1967).